



THE UNIVERSITY OF BRITISH COLUMBIA
FACULTY OF APPLIED SCIENCE

praxim

APSC496 - **Praxim Surgical Robot**

Final Project Report

Faculty Advisor: Antony Hodgson

Nicolas Adams
Davy Chiu
Ibrahim Gadala
David Mountford
Erica Wodzak

Date Submitted:

April 19, 2010

Abstract

Knee replacement surgeries at this time typically require planar cuts that involve removing healthy bone and damaging soft tissue surrounding the area to insert an implant. A trivial solution is to remove only damaged areas of the joint to conserve bone and minimize soft tissue damage; however, that requires precise three-dimensional curvilinear cuts that no existing commercial product can produce accurately, reliably and inexpensively.

Motivation behind this project is to design a solution capable of meeting those requirements based on the dynamic physical constraint concept developed by Nikolai Hungr. The goal is to design a compact, semi-active, haptic interface that can assist a surgeon in making cuts by guiding the cutting tool along a predetermined surface, emulating a realistic hard surface. This report presents the details of the design of the mechanisms and recommendations for future work focusing on the potential accuracy and precision, and user control of the surgical tool.

Results of the project are inconclusive as no prototype was ready for testing and evaluation at the time of writing. A revision including these results will be created once a functional prototype becomes available.

Table of Contents

Abstract.....	i
Table of Figures.....	ii
1.0 Introduction	1
2.0 Project Background.....	2
2.1 Hard Surface Emulation	2
2.2 Dynamic Physical Constraint.....	3
2.3 Existing Device Limitations	3
2.4 Existing Dynamic Physical Constraint Prototype	3
3.0 Project Scope	5
3.1 Requirements and Specifications	5
3.2 Evaluation Criteria.....	5
4.0 Praxia Design.....	7
4.1 Mechanism.....	7
4.2 Size and Weight Optimization.....	8
4.3 Gravity Compensation	9
4.4 Link and Joint Design.....	11
Joint.....	11
Bone Mount Axle (BMA)	12
Rotating Base (RB).....	13
Primary and Secondary Links (PL1 and PL2)	14
Horizontal Offset:.....	15
Link 5 (L5):.....	17

Tool Mount Link:	18
4.5 Error Minimization	19
5.0 Conclusion.....	23
5.1 Device Performance Tests	23
Precision, accuracy and workable area testing	23
Instability.....	24
Results	24
5.2 User Interface	24
Results	24
5.3 Recommendations	24
Controller speed limitations	25
Link Joint Play.....	25
Manufacturing	25
5.4 Conclusion	26
Works Cited.....	27
Appendix A: Limitations of Existing Knee Arthroplasty Devices	29
Appendix B: Link Length Optimization Analysis.....	30
Appendix C: Testing Procedures	35
Appendix D: Manufacturing Drawings.....	40
Appendix E: Encoder Specifications.....	47

Table of Figures

Figure 1: Solidworks rendering of the five link mechanism designed for the Praxim Surgical cadaver prototype	8
Figure 2: Simplified linkage diagram highlighting rotational and linear gravity compensation	10
Figure 3: Cross section of links at joint highlight bearings, encoders and links	12
Figure 4: Model of Praxia's bone mount including the bone mount axle	13
Figure 5: Model of Praxia's rotating base	14
Figure 6: Model of the PL1, PL2, SL1, SL2 that make up the radial link system	15
Figure 7: Model of horizontal offset link	16
Figure 8: Model highlighting encoder position at the joint between link 4 and link 5	17
Figure 9: Model of Link 5	18
Figure 10: Praxia electrical block diagram	21
Figure 11: Functions of each device	21
Figure 12: Weight (lb) vs. Link Length (cm)	33
Figure 13: Axle drawings to be machined on a lathe	40
Figure 14: Additional axle drawings to be machined on a lathe	41
Figure 15: Link drawings to be water jet cut and drilled on a mill	42
Figure 16: The rotating base drawings and vertical offset link designed to be milled	43
Figure 17: Primary links to be water jet cut and machined on a mill	44
Figure 18: Rotating base design.....	45
Figure 19: Secondary links designed to be water jet cut and drilled on a mill.....	46

1.0 Introduction

Praxia is the name given to the surgical tool design described in this document. The tool is a 3-dimensional haptic interface device used for curvilinear surface generation in surgical procedures, particularly knee replacement procedures. The development of the Praxia prototype is a continuation of work in curvilinear surface generation using haptic devices completed at The University of British Columbia (UBC) by Nikolai Hungr.

Prior to Praxia, three-dimensional hard surface generation has been demonstrated and used in various applications; Praxia's aim is to redevelop previous designs, incorporating the additional features necessary to implement the device in a surgical environment, and to subsequently assess it from the user's (surgeon's) perspective. The purpose of this project, and thus the device, is to minimize soft tissue damage during uni-compartmental knee arthroplasty (UKA) procedures by developing semi-active, bone-mounted cutting guides.

Three parties are involved with the current project: Dr. Christopher Plaskos of Praxim, Dr. Antony Hodgson, a member of the Faculty of Engineering at UBC, and 5 students from the APSC 496 class at UBC. With this device, Praxim aims to target high-volume arthroplasty hospitals that perform multiple UKA procedures per day that will use the Praxia, alongside Praxim's Nanostation navigation system, as a low cost alternative to technologies that integrate with Computed Tomography. A further application of the device is implementation in lower-volume facilities where surgeons perform UKAs on a less-frequent basis and thus have less experience with the procedure. In this situation, Praxia will allow for a more structured procedure, providing assistance to the surgeon and ensuring a higher precision and less tissue damage.

This report describes key features of the design developed for the Praxia prototype, and provides an assessment of the performance of the design, discussing future work needed to develop a commercial device.

2.0 Project Background

The orthopaedic surgery community continuously searches for new surgical techniques to minimize tissue removal, which will subsequently decrease patient recovery time and improve the quality of the surgery. Haptic devices provide one such technique, and have been used previously to implement bone-conserving implants in UKA by improving the control and accuracy of the surgeon during the procedure. Haptic devices achieve this by emulating a hard surface that can be used as a barrier-guide for the surgeon when performing operations, thereby minimizing the potential damage to soft tissue and providing the opportunities to use implants customized to individual patients by adapting the hard surface to only remove regions of arthritic bone.

Work completed prior to the development of the Praxia prototype focused on hard surface emulation of curvilinear surfaces with applications to knee arthroplasty (Hung, 2008). The current project builds on designs developed by Nikolai Hung, as well as work done by a previous team of UBC students, to attempt to implement three-dimensional hard surface emulation of curvilinear surfaces in surgical applications.

This section briefly introduces the concept of hard surface emulation and the dynamic physical constraint developed by Nikolai Hung, summarizing the limitations of existing technologies designed for the same application.

2.1 Hard Surface Emulation

Hard surface emulation is useful in orthopaedic surgeries as it restricts all bone milling and cutting to critical areas, having limited impact on all other aspects of the surgery. The result is a device that allows free motion of the cutting tool away from the virtual surface, yet impedes movement of the tool past this surface (i.e. in areas where critical damage could occur). A curvilinear surface can be implemented to optimize cutting techniques by accurately restricting the cutting tool from entering sensitive

regions of bone and tissue, permitting the removal of only undesirable or arthritic bone during the procedure. Ideally, feedback generated by the haptic device should only impede the user at the desired the surface, and otherwise seem non-existent.

2.2 Dynamic Physical Constraint

The dynamic physical constraint mechanism, developed by Hungr, utilizes a constraint that can be repositioned continuously to impede the motion of the end-effector, maintaining it at position of a specified distance away from emulated surface; this concept provides the user with complete freedom of motion when not in contact with the hard surface. By updating the position of the hard constraint based on the position of the end-effector, a surface can be emulated by the device. The hard constraint is implemented with a physical stopper-mechanism, which ensures that surface is created with infinite stiffness and allows the user to trace a continuous surface.

2.3 Existing Device Limitations

A number of devices, many of which are commercial technologies, have been designed to aid in orthopaedic surgeries by restricting tool motion. Appendix A: Limitations of Existing Knee Arthroplasty Devices summarises the limitations of many of these devices.

Numerous reports identify complications related to surgeries completed with existing bone shaping devices. These failures include problems relating to device-bone mounting and excessive stress at mount connections, significant misalignment of critical bone joints and failure of implants due to improper placement. These failures directly relate to the performance of the bone shaping devices, specifically the device accuracy and precision. Mechanical misalignment, specifically loosening of mechanical joints, is often identified as the underlying cause of these failures.

2.4 Existing Dynamic Physical Constraint Prototype

A prototype implementing the dynamic physical constraint mechanism (developed by a UBC student team in 2008) proves that the mechanism effectively implements a hard surface. This prototype however has a number of limitations.

Surface Instability

The prototype makes minor adjustments without any changes in tool position causing instability at the far edges of the operating surface and at sharp corners. This instability significantly reduces the user's sense of control.

Freedom Away from Virtual Surface

The user must support the weight of the device throughout operation. This significantly inhibits motion and makes control of the end-effector difficult and the device unusable. The majority of the weight is the result of a linear bearing and the position of the motor.

Material Selection

The design is constructed from aluminium which cannot be sterilized. The links have also been sized based on the bearing selection and make the prototype significantly larger than necessary.

Controller Design

All the processing is performed on a 16 MHz microcontroller incapable of achieving the necessary speed due to the lack of a Floating Point Unit.

3.0 Project Scope

The aim of the project was to redesign the hardware and software of an existing three-dimensional haptic interface device to produce a prototype that implements a dynamic physical constraint mechanism in a surgical environment. The prototype's performance was to be assessed through user tests based upon the device's ability to emulate a hard surface and the degree to which it impedes user movement. The end goal for the prototype's development was to be ready for cadaver testing in the spring of 2010; all design decisions for the prototype were to be made considering application of the device in a sterile surgical environment.

3.1 Requirements and Specifications

Requirements and specifications for the project were developed based upon the limitations of previous iterations of the project, client goals and objectives, and failures seen in alternative technologies designed for TKAs. Three key specifications governed the majority of design decisions made through the course of the project:

1. The device's hard surface constraint must be physically imposed within 0.5mm of the desired "physical" surface
2. The device must be able to be solidly mounted on the femur during surgery, and completely secured with minimal movement (+/- 0.5mm)
3. The device must weigh less than 5 lbs in total
4. The device's resistance to user-directed movement away from the hard surface must be less than 10N

3.2 Evaluation Criteria

A user assessment of a surgical aid such as the Praxia can be divided into two categories; (1) device precision and accuracy and (2) user feel and control.

In order to be considered for any surgical procedure, the device must deliver results that meet or exceed the accuracy needed in a surgical procedure. In this case, performance relates to the effective position of the generated hard surface relative to the desired position of the surface. Device precision and accuracy is affected by the rigidity of the mechanical components, the device's mechanical design, the accuracy of the position measurements of the surgical tool, and the reliability with which the hard constraint can be repositioned based on potential user movement. The project requirements specify that the total error generated by mechanical play and encoder position readouts must be less than 0.5mm, and that the total error in the connection between the device and the operating surface should be less than 0.5mm. This amounts to a total precision of +/-1mm.

The user feel and control of the device cannot be quantified as easily as precision, but an assessment of user feel must consider the ease and consistency with which an operator can position the tool. Two device characteristics have been identified as potentially influencing the user feel and control of the device. Unlike the majority of tools used in surgical procedures where the force exerted on user is always in the same direction (due to gravity), haptic interfaces create a situation where the force can vary based on the position and orientation of the tool. Forces too large to be easily supported by the user, or forces that vary in an unpredictable manner, will have a negative impact on the feel of the device, which limits the user's acceptance of the device, potentially rendering it useless.

4.0 Praxia Design

Engineering analysis and design completed in the development of the Praxia device focuses primarily on the basic layout and design of the mechanism that will be used to implement the hard constraint and improving the speed of the system by using a microprocessor that can perform floating-point operations. The design presented here redevelops the four-link mechanism previously used by placing the hard constraint and the motor at the base of the device, where the device is mounted to the bone. Significant effort has also gone into minimizing the size and weight of the device, while still using strong materials that can be effectively sterilized. This section describes the device's design and design decisions that have been made, starting with an overview of the mechanism, and finishing with the device's link and joint designs.

4.1 Mechanism

The mechanism developed for the Praxia prototype is pictured in Figure 1. It combines a radial link system (RLS) comprised of the primary links that implements the hard constraint and the secondary links that constrain the primary link system (PLS) to linear motion. The PLS is free to rotate about the y-axis at the Rotating Base Axle (RBA), and is attached to link 3. Link 5 is attached to link 4 and rotates freely about the x-axis, positioning the tool head, which is connected to the device by the tool mount (TM). The TM positions the tool head at the centre of the radius.

The position of the tool head is determined by three encoders placed on the rotating base (RB) – not pictured -, at the joint between the primary links of the RLS, and at the joint between links 4 and 5. The hard constraint motor sets the position of the hard constraint that, when activated, restricts the motion of the primary link toward the RB.

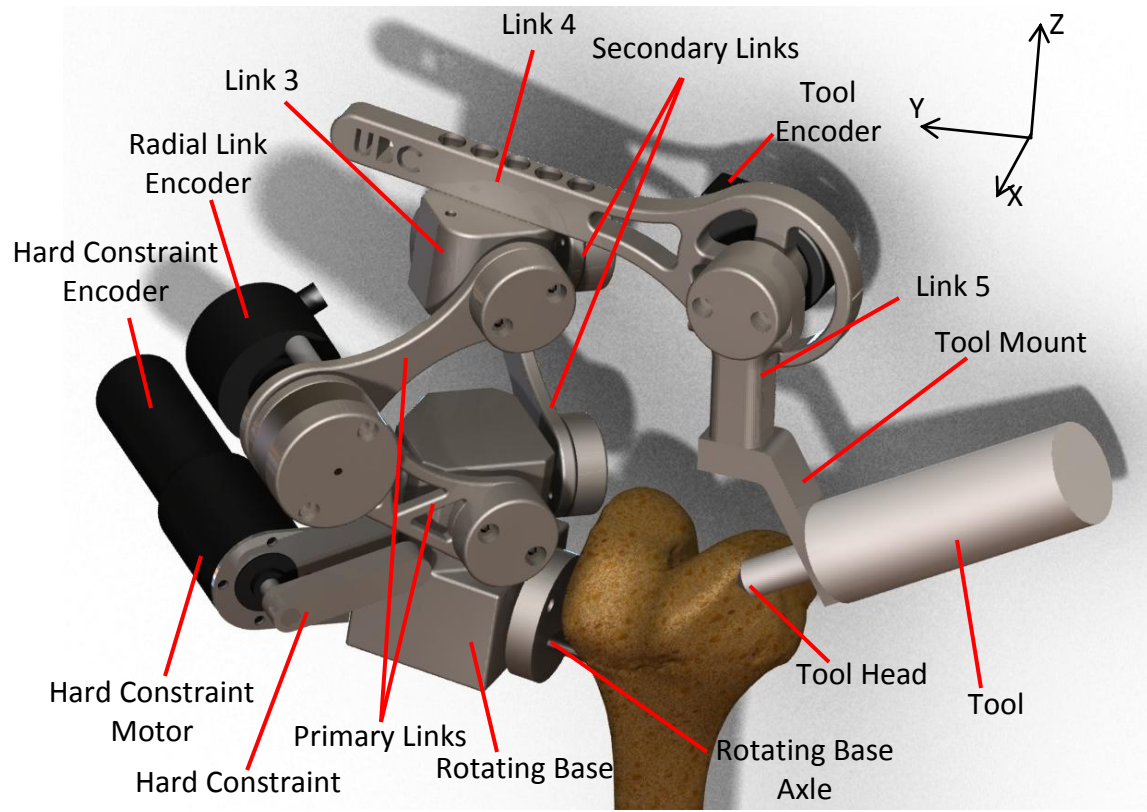


Figure 1: Solidworks rendering of the five link mechanism designed for the Praxim Surgical cadaver prototype

4.2 Size and Weight Optimization

The operating workspace and total weight of the device are two critical characteristics that ultimately determine the overall success of the design. Analysis was performed to maximize the potential workable area of the device by adjusting link lengths, while keeping the total weight of the device within the design requirements.

There are two critical parameters that must be adhered to in Praxia's design: minimum workable area with a diameter of 63.5mm and a maximum total device weight of 5lbs. Any increase in workable area or decrease in the total weight of the device is beneficial to the design of the system, however the opposite is detrimental. The final link lengths, shown in Table 1, were determined by maximizing the total allowable workable area while maintaining the weight of the links at approximately 2lbs.

Link	Length [cm]
1	7
2	7
3	5
4	5
5	7

Table 1: Final design link lengths

Joint Angle	Range [degrees]
$\Theta_{12 \text{ min}}$	30
$\Theta_{12 \text{ max}}$	120
$\Theta_{54 \text{ max}}$	45
Θ_3	20
Θ_{135}	-15

Table 2: Joint operating range (see Appendix B: Link Length Optimization Analysis for a joint angle reference diagram)

With the above link characteristics, the device has a workable area of 90mm. This range has been optimized based on the user requirements determined earlier on in the project. The length has also been selected to ensure that there is no interference between radial link encoder and the hard constraint motor. Testing the Praxia prototype will further assess the user feel based on weight, and may require a reduction in the potential workable area in order to reduce the total link weight, thus improving the user's level of satisfaction with the device. The complete link length optimization is included in Appendix B: Link Length Optimization Analysis.

4.3 Gravity Compensation

One of the primary focuses of the new design is to improve the user's "feel" of the device (i.e. how cumbersome vs. how comfortable it may be to use). A critical design parameter of this criterion is the weight of the device (including the weight of the tool) that the user must support when the tool tip is away from the hard surface. Gravity compensation mechanisms can be implemented to transfer this load from the user to

the support structure and bone mount. Two types of gravity compensation implementations were considered, and are as follows:

- **Rotational gravity compensation** that counteracts moments produced about the bone mount due to the weight and position of the device
- **Linear gravity compensation** that resists motion towards the bone mount, causing the radial link system to collapse

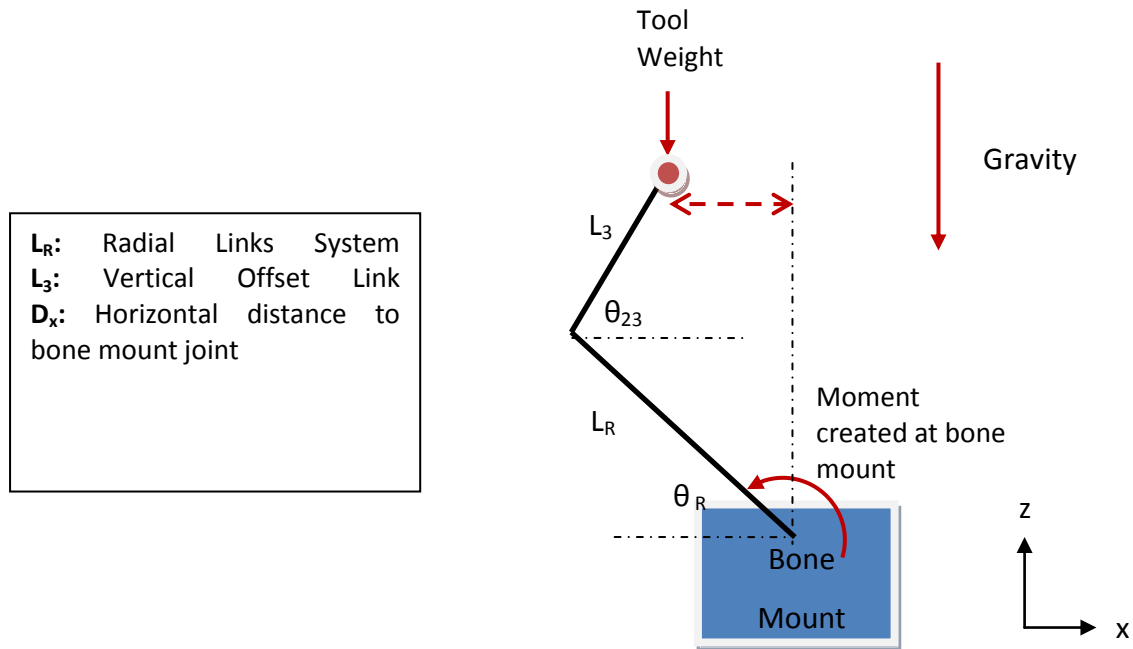


Figure 2: Simplified linkage diagram highlighting rotational and linear gravity compensation

A technical assessment of rotational gravity compensation suggests that for the theoretical weight of the device, rotational gravity compensation is not necessary, and thus no rotational gravity compensation mechanism was designed. This assessment must be verified with user tests using a completed prototype.

Linear gravity compensation has been implemented by a tension spring mechanism that extends along the secondary support links of the radial link system. A simple position adjustment mechanism coupled to the rotating base facilitates fine spring tension tuning that will be optimized based on user feedback. User tests of the prototype will be used to optimize the spring tension for the desired operating range.

4.4 Link and Joint Design

The detailed design goals for the Praxia's mechanical design are driven by the need to create a device that is lightweight and small enough to provide adequate user feel while minimizing the force exerted on the bone; furthermore, the device must meet all performance goals. As a result the joints have been designed using minimum constraint theory, and measures have been taken to ensure that the joints do not become loose over time. The Praxia prototype has been constructed from 303 stainless steel and is designed to integrate with Praxim's bone mount. This section will discuss the major functions and provide an overview of the design for each component.

Joint

Functions

The primary functions of each joint are to act as the point of connection between two links and to mount the encoders to allow the encoder shaft to rotate with respect to one of the links.

Design Goals

- Allow bearings to be spaced apart to minimize play by in the joint – total play must be kept below 0.1 degrees
- Reduce possibility of joint becoming loose
- Minimize the joint size to avoid interference between components

Design Features

Figure 3 shows the basic joint layout for the Praxia prototype. The encoder shaft screws into the preload cap and is rigidly attached to one of the links to allow for relative motion. The preload cap is combined with spring loaded washers to reduce the tendency of the joint to become loose. The bearings have been spaced but kept small to reduce the total size of the joint.

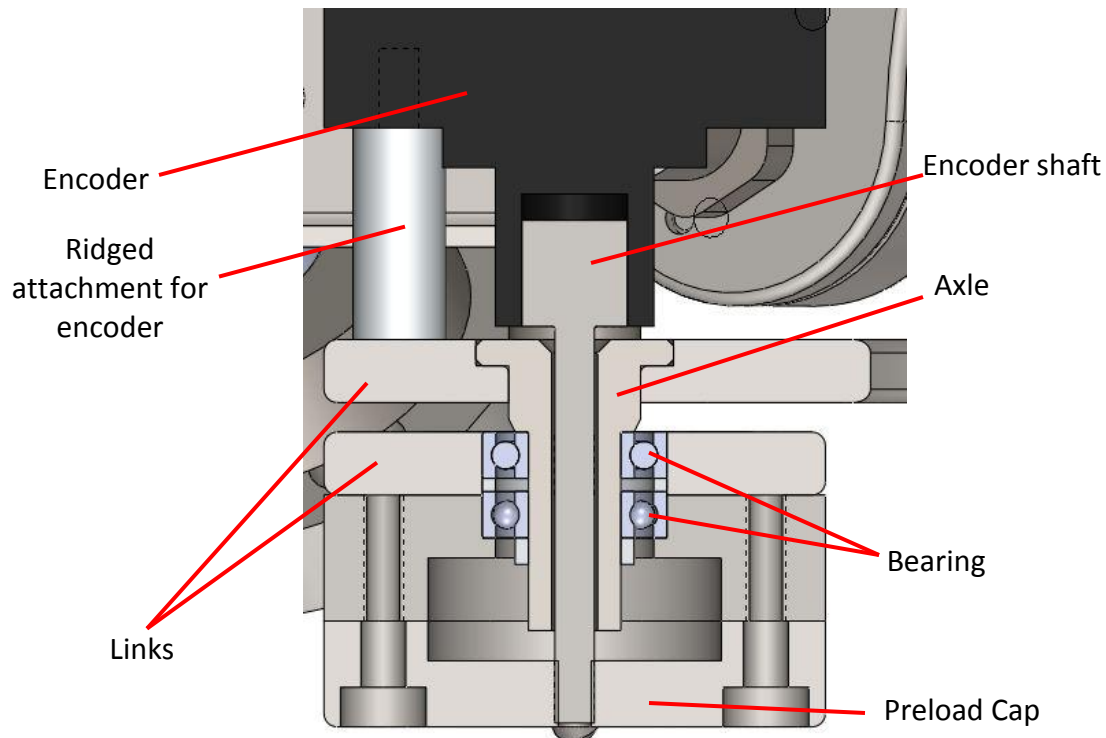


Figure 3: Cross section of links at joint highlight bearings, encoders and links

Bone Mount Axle (BMA)

Functions

The bone mount axle must attach to Praxim's adjustable bone mount and allow the rotating base to freely move around it. The axle must be rigidly coupled to the encoder shaft, as the shaft determines the orientation of the rotating base with respect to the bone.

Design Goals

- The bearings for the rotating base must be spaced as far apart as possible to minimize play in the joint
- Recess caps to minimize the size

Design Features

Figure 4 shows the bone mount and rotating base axle design for the Praxia prototype. The bone mount pictured is completely compatible with Praxim's bone mount and the axle consists of a shaft and a shoulder and allows for 30mm between bearings.



Figure 4: Model of Praxia's bone mount including the bone mount axle

Rotating Base (RB)

Functions

The RB is the base attachment for the device. The RB couples the primary and secondary links for the radial linkage system to the BMA, and also securing the hard constraint motor and BM encoder to the device.

Design Goals

- Design to be as easily manufactured as possible
- Remove any unnecessary weight from the rest of the device, housing heavy components here

Design Features

Link axles are designed to be threaded into the RB in order to avoid press fitting. The attachment points for the links, shown in Figure 5 are perpendicular to each other and angled 45 degrees away from the BMA to minimize interference with the soft tissue around the knee.

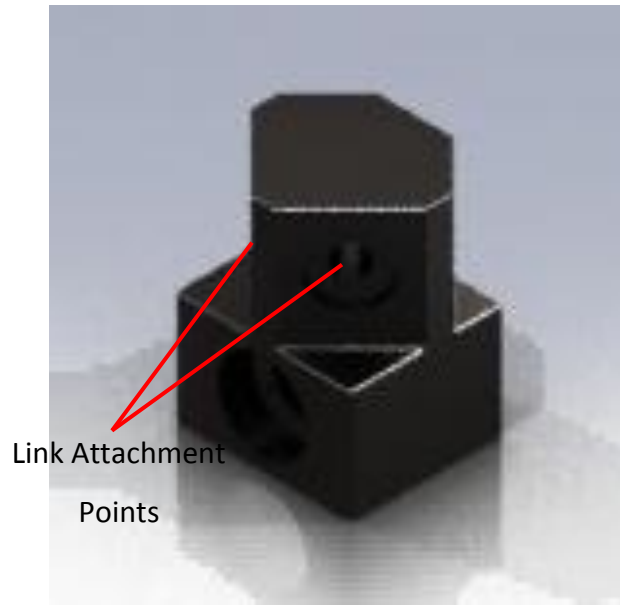


Figure 5: Model of Praxia's rotating base

Recommended Improvements

Casting this part would allow for more complicated geometry, which in turn may reduce the total amount of material required to accomplish its required functions and therefore reducing the weight of the part.

Primary and Secondary Links (PL1 and PL2)

Functions

The primary and secondary links combine to generate a radial link system that constrains the upper connection block (link 3) to move linearly with respect to the RB. The primary links facilitates the physical constraint preventing motion past a defined linear distance between the RB and link 3.

Design Goals

- Minimize the size and weight of the links
- Accept hard constraint at PL1
- Implement shape that simplifies the motor positioning function
- Minimize the size of the joints between the two primary links and the two secondary links

Design Features



Figure 6: Model of the PL1, PL2, SL1, SL2 that make up the radial link system

Link Size:

The physical constraint function is simplified by keeping the primary links equal in length and size. 70mm links provide the necessary operating envelope and reduce the possibility of collisions between the primary link encoder and the physical constraint motor.

Link Profile:

All of the links, except PL1, have a peanut shape in order to reduce the weight of the links. PL1 has the peanut profile on the top half of the link, but the bottom half of the link is a straight edge in order to provide an edge for the physical constraint to act upon.

Recommended Improvements

The joints have been designed to be as small as possible while still providing minimal play, but a possible improvement to the design would be to simplify the machining process for these links as much as possible. Simplifying the joint design could lead to a much easier and faster assembly of the device, and reduce critical tolerances by minimizing machining error.

Horizontal Offset:

Functions

The horizontal offset acts as a connection between the up-down motion of the primary links and the rotational motion of the links on which the tool is mounted on.

The horizontal attachment is rigidly fixed to the upper rotating block on one end, and is coupled with link 5 (tool mount link) on the other. The coupling with the tool mount link incorporates an encoder, to be able to determine the position of the tool bit at all times.

Design Goals

- Rigidity is crucial, as any deflection is a direct intrusion into the hard surface
- Remove unnecessary weight
- Allow for multiple lengths to cater to different surgical requirements

Design Features

The link is designed to be mounted above the upper rotating block with hex cap screws. An array of predrilled holes will allow for the interchanging of the link length depending on the surgery. On the tool mount side, the link width expands to a circular shape to allow for the mounting of an encoder on the back side. A through-hole is made so that the encoder shaft can interact with the tool mount link on the front side.



Figure 7: Model of horizontal offset link

Recommended Improvements

A reduction in the link size can be achieved if a smaller encoder that meets the required precision and mounting orientation is available. Also, a more convenient length interchanging design could be implemented, which can allow “on-the-fly” length changes during the surgery itself, rather than dismantling the whole link and assembling it to the new length.



Figure 8: Model highlighting encoder position at the joint between link 4 and link 5

Link 5 (L5):

Functions

Link 5 is a crucial part of the design, as it significantly increases the flexibility of the system and allows the tool head to track the hard surface effectively. Link 5 rotates about a shaft which is coaxial to the encoder shaft running through the horizontal offset. Thus, link 5 rotates in a plane parallel to the horizontal offset link. The movement of link 5 adds width and depth to the workable area.

Design Goals

- Minimize resistance to user movement (as smooth as possible)
- Remove unnecessary weight
- Reduce size, without compromising load-bearing capability

Design Features

The link is designed as a downward vertical addition to the horizontal offset and allows rotation about the joint shaft between the two links. It comprises of two parts,

the actual vertical link, and the cap. The link itself tackles the main functionality of providing a downward vertical arm for the robot, while the cap houses the bearing assembly (for smooth motion) and serves as the end-mount for the encoder shaft. Since the encoder is mounted on the “static” horizontal offset, the motion of link 5 can be determined by simply measuring the rotation of the encoder shaft.



Figure 9: Model of Link 5

Recommended Improvements

An amalgamation of link 5 and the tool mount link (described below) could allow for a more compact and light weight design.

Tool Mount Link:

Functions

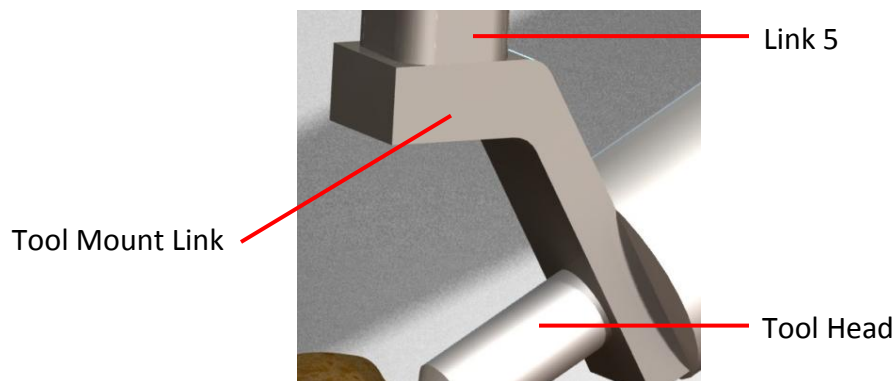
The tool mount link is the final link of the design and is the one on which the surgical tool is mounted. The link allows for rotation about the axis of link 5, thus giving the surgeon the ability to hold the tool from virtually any angle. The tool mount link does not allow translational movement in itself, however, as it is attached to link 5 and the rest of the structure, it also moves in the up-down direction as allowed by the primary links.

Design Goals

- Full 360° freedom rotation about the link 5 axis
- Maintain structural integrity while bearing the full weight of the tool

Design Features

The tool mount link is designed to couple with bottom of link 5 with a joint fastener (shoulder screw) that threads into link 5, providing the necessary constraint against translational movement and allowing free rotational movement. The interface between the link and the tool is at an angle in order for the tool bit to always touch the cutting surface using its side, for optimal cutting performance.



Recommended Improvements

Making the tool rotate with respect to the tool mount link lets the surgeon's hand follow a more natural and comfortable sculpting motion. This additional degree of freedom does not improve the function of Praxia itself, but allows the surgeon to be less constrained and more relaxed during the surgical procedure.

4.5 Error Minimization

For the device to be practical, the result of the assisted cut must maintain implant frontal plane alignment accuracy to within 3°, meaning that the physical restraint must prevent no more than 1mm of penetration (Plaskos, 2005). The physical constraint must also respond with sufficient speed, at a rate of 1 kHz (Hung, 2008). The precision and accuracy of the device is limited by encoder resolution and update speed, as well as mechanical play discussed previously.

To achieve less than 0.5mm of penetration, the encoders have been selected to provide the highest precision in the smallest sizes available. Table 3 shows the details of the encoders and the respective links that they are attached to. Full specifications can be found in the appendices.

Table 3: Encoder models and resolutions

Rotating Base	1000PPR (4,000 effective CPR) – AME-1000V-T600K
Links 1-2	2500PPR (10,000 effective CPR) – TRD-SH2500VD
Links 4-5	1000PPR (4,000 effective CPR) – AME-1000V-T600K

Using this combination of encoders, surface penetration is limited to an absolute theoretical maximum of 0.166mm relative to the axle of the bone mount.

To achieve an update rate of 1 kHz, a 600 MHz microprocessor with an FPU (Floating-Point Unit) is selected to perform all the data processing. The previous group of students had all the processing performed on a 16 MHz microcontroller; however, analysis in the Technical Analysis Report shows that this microcontroller is incapable of achieving the necessary speed due to the lack of an FPU. The microcontroller from the previous has been kept to serve as an interface between the microprocessor and the encoders/motor to reduce development time. Figure 10 shows an overview of how the devices are connected.

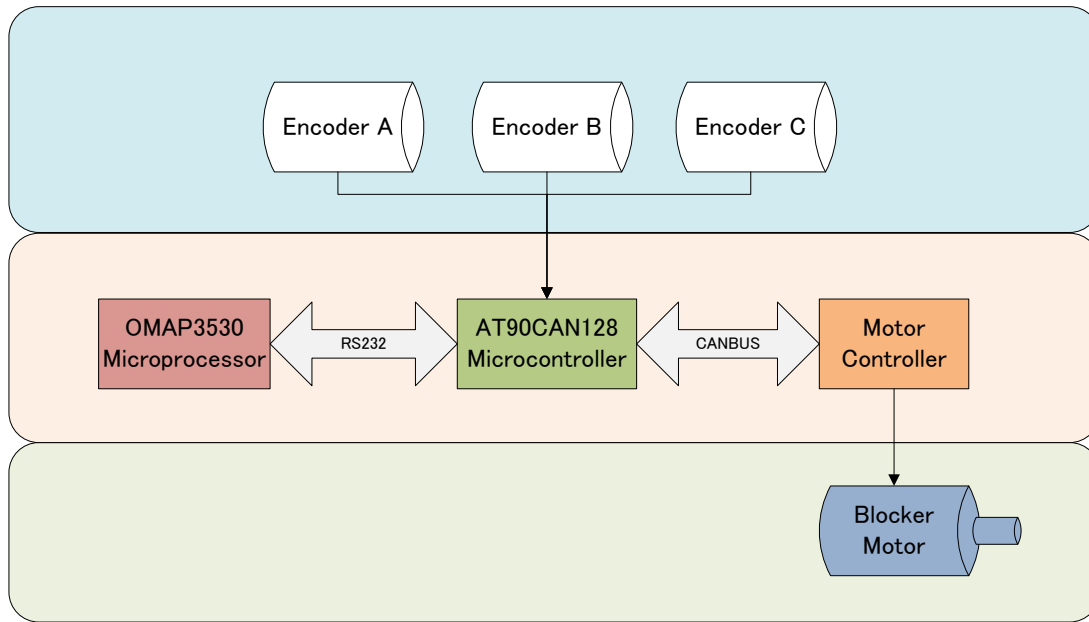


Figure 10: Praxia electrical block diagram

The OMAP3530 microprocessor is connected to the AT90CAN128 microcontroller via RS232 serial interface at 57600 baud. The microcontroller keeps track of the positions of the encoders and transmits them to the OMAP3530, which determines where the end-effector is relative to the virtual surface using forward kinematics. A blocker position is then calculated and transmitted to the microcontroller, where it is then relayed to the motor controller via the CAN interface. Surfaces are pre-programmed with equations for simplicity.

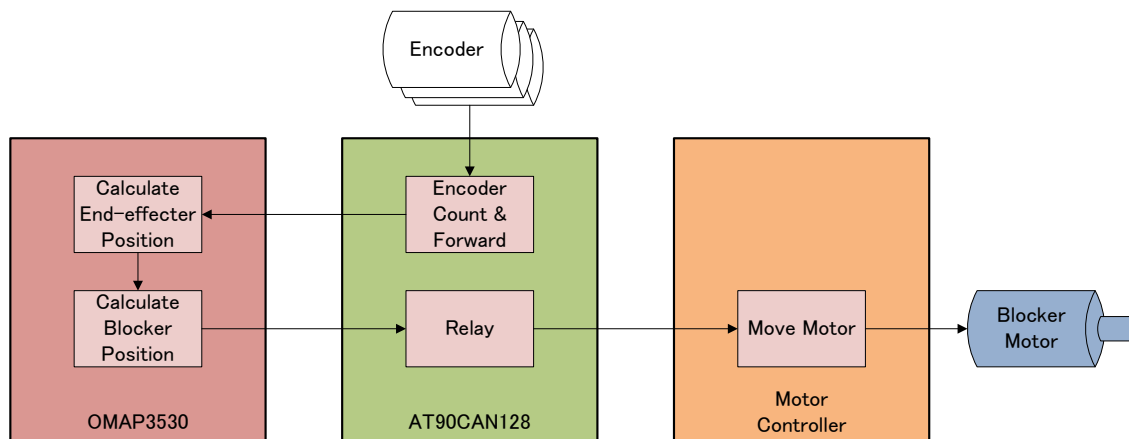


Figure 11: Functions of each device

The QNX Neutrino operating system has been selected to run on the OMAP3530 for its real-time guarantee for applications running on embedded systems. It also provides a developer-friendly environment to develop and debug applications over serial or Ethernet.

5.0 Conclusion

The two primary concept goals the Praxia prototype must meet in order to implement an effective surgical tool for UKAs are as follows:

1. Device Performance: Does the device perform the required tasks specified in design conceptualization?
2. User Interface: Is the device user-friendly? How well does the device interact with the user?

Tests have been designed to evaluate the prototype design based on these goals.

5.1 Device Performance Tests

The device performance tests determine whether the device will provide the precision and accuracy necessary to be considered an acceptable surgical aid. Concept specifications require the hard surface constraint to be physically imposed within 0.5mm of the desired model surface. This means that the device must recognize the current position of the tool, within a 0.5mm tolerance, based on all encoder readings and any play in linkage joints. The device must also provide a total workspace large enough to install a common uni-compartmental knee implant. This implant can be approximated as a circle with a radius of 63.6mm.

Precision, accuracy and workable area testing

In order to assess the precision of the device, the position/location of a number of points on Praxia must be known to a greater accuracy than the required precision of the device. This is achieved by using a mill with a known accuracy of $\pm 0.05\text{mm}$ to locate and mark four calibration positions on a piece of carbon steel with a coefficient of linear expansion of $13.0\text{E-}6 \text{ m/m K}$. Allowing for a 100K temperature variation, the mark positions will be known within $\pm 0.05\text{mm}$. The device accuracy can be determined by comparing the device location with the actual position of the milled marks.

Instability

Tests of previous prototypes identify the presence of instabilities at discontinuous positions (corners and locations where two curves meet) and near the edge of the hard surface. The effective position of the hard surface position and any potential instability can be determined by tracing the outline of various hard surfaces and attempting to penetrate the hard surface.

Results

Testing has not been completed

5.2 User Interface

The user feel of the device is essential for widespread acceptance, and has been a major focus of the current design. Previous prototypes confirm that 3D haptic surfaces can be implemented, but prove difficult to control due to a resistance to user movement (termed “virtual weight”). User-based tests will be used to determine the effectiveness of the device as a bone sculpting tool.

Results

Testing has not been completed

5.3 Recommendations

User tests and performance evaluations have not been completed because the prototype is not yet fully functional. Basic performance tests have been used to evaluate the encoder performance based on the update speed and the consistency of each reading, and the software has been verified using hand calculations. The majority of the mechanical aspects of the design require user tests, but an evaluation of the manufacturing techniques and individual joint design can be provided based on machining and fabrication analysis. Once prototype construction and user tests have been completed, a review of the prototype will be presented to the client and a formal list of recommendations will be compiled from the findings.

Controller speed limitations

Due to the speed limitations of the RS232 serial interface, the overall speed of the system can only achieve 90% of the 1 kHz requirement at 900Hz. One solution is to use a faster interface such as the Two-wire interface. For a production system, a better solution is to use a single microcontroller capable of processing floating-point math. The TI Stellaris with an ARM Cortex M4 core is a good candidate.

Tests show that the microcontroller is able to detect 100% of repositions of the encoders and will position the tool within 0.166mm of the desired location if mechanical play is ignored. This allows for 0.344 mm of additional error from the bone mount joint, play at the links. The design uses relative encoders and the total performance may be limited by accuracy of the calibration position as a result. The calibration position accuracy will not be known until the prototype has been completely manufactured.

The software implemented uses encoder inputs to compute the desired user and hard constraint position based on the implemented model. Errors occur due to rounding in the position identification and bugs in the software. No errors have been found in current version of the code and all variables maintain 53 digits, so there is negligible error in the software as a result.

Link Joint Play

Manufacture of the prototype has been rushed, resulting in a significant increase in play in the joints. An assessment of the maximum in the primary hard constraint joints shows play in the joints of approximately 1 degree, amounting to +/-2mm of error. Combining the primary and secondary links to create the radial link structure reduces the error to 1mm; however this error is unacceptable for surgical purposes. Manufacturing techniques must be considered further to ensure the desired tolerances for critical components can be met.

Manufacturing

Manufacturing of the prototype has been completed using a combination of water jet cutting and machining. The complexity of the links necessary to reduce the overall

weight of the system makes accurate machining difficult. As a result, a combination of casting and CNC is recommended for additional devices. Casting should be used for the rotating base and the tool mount while minor changes made to the current design could allow for complete manufactured using water jet and CNC. Component specific recommendations have been included in the detailed mechanical design section. Manufacturing drawings are included in the appendices.

5.4 Conclusion

The design presented in this document for the Praxia has not successfully fulfilled the project requirements due to difficulties in manufacturing the prototype. A prototype will be constructed, but is likely to lack the machining precision necessary to effectively assess the precision and accuracy. User tests will be conducted and compiled to assess the weight and potential gravity compensation features. Results of these tests will be added to future revisions of this document.

Works Cited

Hayward, V., & MacLean, K. E. (2007). Do It Yourself Haptics, Part I. *IEEE Robotics and Automation Magazine* .

Hungr, N. A. (2008). Haptic Emulation of Hard Surfaces with Applications to Orthopaedic Surgery. Vancouver, British Columbia, Canada: University of British Columbia.

Kuchenbecker, K. J., Fiene, J., & Niemeyer, G. (2006, March). Improving Contact Realism Through Event-Based Haptic Feedback. *IEEE Transactions on Visualization and Computer Graphics* , pp. 12(2):219-229.

Lawrence, D. A., & D, C. J. (1994). Performance Tradeoffs for Hand Controller Design. *Proceedings of the 1994 IEEE International Conference on Robotics and Automation*, (pp. 4:3211-3216).

Plaskos, C. (2005). *Modeling and Design of Robotized Tools and Milling Techniques* .

Salisbury, K., Brock, D., Massie, T., Swarup, N., & C, Z. (1995). Haptic Rendering: Programming Touch Interaction with Virtual Objects. *Proceedings of the 1995 Symposium on Interactive 3D Graphics*, (pp. 123-130).

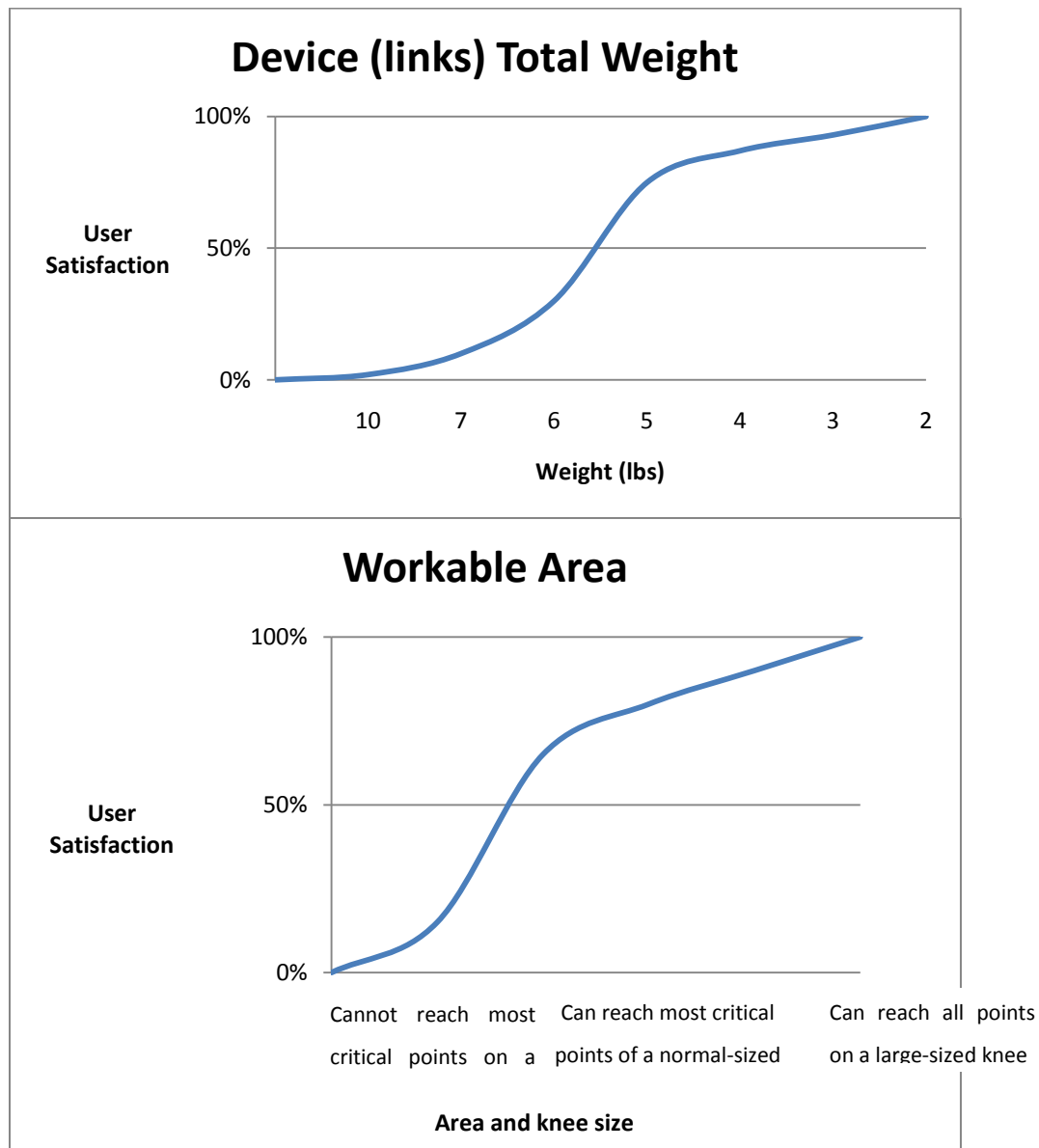
Appendix A: Limitations of Existing Knee Arthroplasty Devices

The following is a list of failures of existing knee arthroplasty surgical aids:

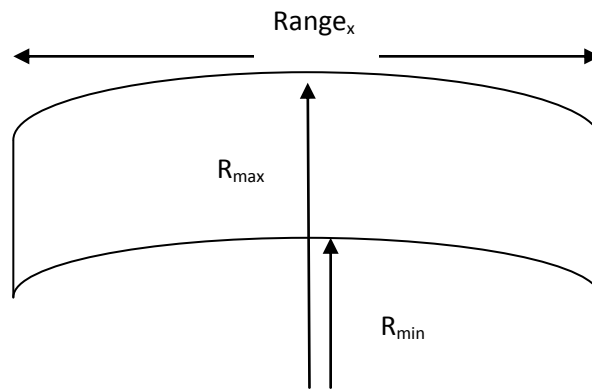
- Bone damage due to improper surgical procedure or excessive forces causing mechanical failure in the device or the bone structure
- Loosening of device components (any or all) due to improper device placement or fastening or due to forces exceeding the tolerance threshold of the device post-operation (implants)
- Allergic reaction to any of the device components or elements which the body is exposed to during the implantation procedure
- Infection related to surgery from improper sterilization of equipment or the surgical environment or improper sterile practices of the surgical staff
- Loss of neurological function or impairment of neurological function due to insults or obstructions to the nervous system (during surgery and after completion)
- Cardiovascular damage, including hemorrhage from improper healing during or post-operation as well as damage to bone vasculature
- Mechanical failure of the device such as loosening of its connection(s) with the bones.
- Early failure of implant due to asymmetric loading, which is a direct cause of inaccurate bone-shaping and/or referencing
- Poor knee mechanics and/or loosening of the components due to improper implant alignment with respect to bones and soft tissues (direct cause of inaccurate surface shaping)

Appendix B: Link Length Optimization Analysis

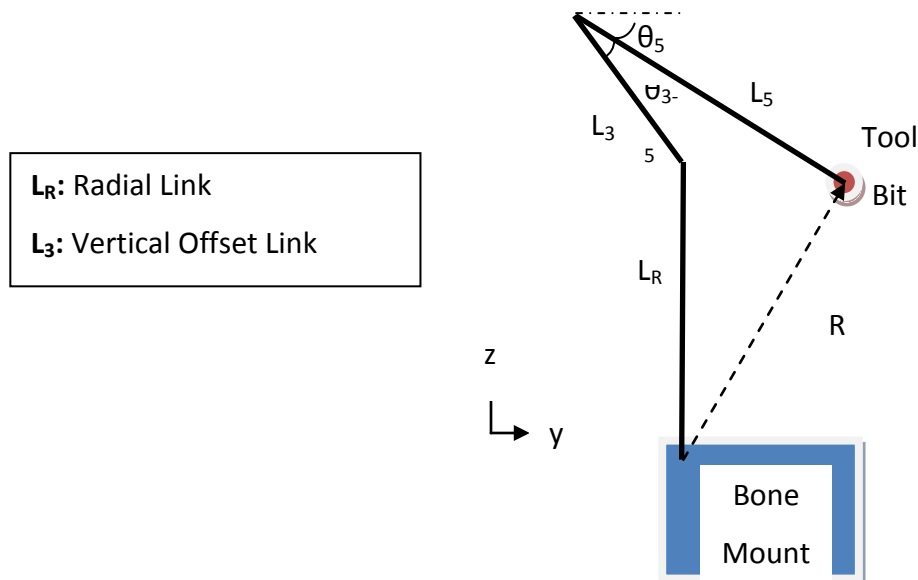
An essential calculation which had to be completed before moving on to other analyses is that of the linkage lengths (most importantly Link1 and Link 2) and their corresponding “workable” area. In this analysis, we try to maximize the link lengths to maximize the workable area which can be sculpted using the tool bit. At the same time, the link sizes should not be too large in order to minimize size and weight of the overall device. Thus, a balance must be struck between link sizes and workable area. The following user satisfaction curves illustrate the relative importance of each:



From the graphs, it can be seen that the link weights are slightly more important for user satisfaction, and thus, the structural design focus will be to reduce link size (and weight) more than to achieve a larger workable area than what's functionally needed. This section of the report explains the theory behind the link size calculations and how we determined them to be within discrete ranges. First of all we must define how we express the workable area at the tool bit. From the *Matlab* plots results discussed in the CFP, we already know the general shape of these areas. They can be *approximated* as the area between two circular boundaries, one boundary of which is larger than the other. Thus, we define the outer or larger curved boundary as R_{\max} and the inner or smaller curved boundary as R_{\min} . The side boundaries of the workable area are approximated as straight vertical lines, and the distance between them is called Range_x . Thus, the workable area looks like the following (note: in reality, the origins of the radii should be different, but this is a very close approximation):



With the workspace coordinates defined, we must also define the variables of the linkage design in order to optimize the linkage sizes. The linkage variables are vital for the analysis and are defined in the figure below. The figure is a simplified illustration of the linkage orientation, with the square point representing the bone mount and the circular point representing the cutting tool. The legend to the left identifies the link names.



With the configuration above, we need to maximize the workable area while, at the same time, minimizing link lengths. The goal of the following analysis is to optimize the link lengths and workable area. We perform the analysis by first computing a mathematical relationship of the workable area based on the link lengths and angles defined in the figure above.

To start, we write the following geometric relationships between distances and angles:
 $L_R^2 = L_1^2 + L_2^2 - 2 L_1 L_2 \cos \theta_{12}$ (note: L_1 , L_2 and θ_{12} are not shown in the diagram)
 We will create a virtual length called L_5 ;

$$L_5 = L_5 \cos \theta_5$$

With that new virtual length, we can define the “reachable” length in the “z” and “y” directions stated above:

$$z = L_R + L_3 \cos \theta_3 - L'_5 \cos (90 - \theta_3 - \theta_{3-5})$$

$$y = -L_3 \cos \theta_3 + L'_5 \cos (90 - \theta_3 - \theta_{3-5})$$

Since the “z” and “y” lengths described above are components of the R vector, we can compute the length of R simply as follows:

$$R = \sqrt{z^2 + y^2}$$

R is the range vector which characterizes the size of the workable area in our analysis.

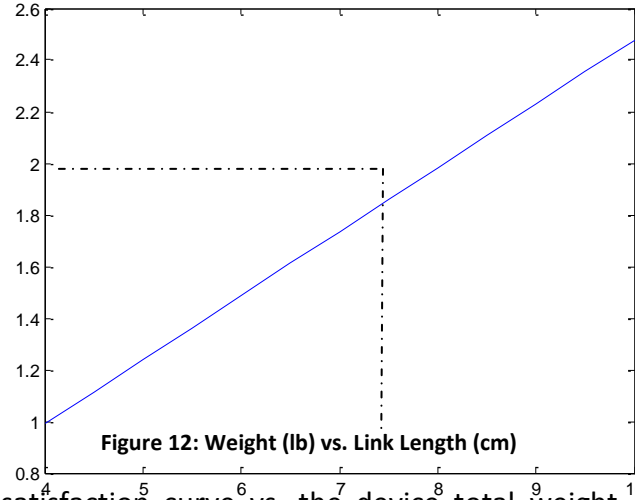
Knowing the mathematical relationship between link lengths (sizes) and workable area, our task is to find an optimized combination, which gives us both a satisfactory workable area and a reasonable size and weight for the device. We do so with an excel spreadsheet. We insert the variables and equations above into the spreadsheet, and observe the change in workable area based on links 1 and 2. It is known that the workable area increases with increasing link sizes, however, our goal was to pinpoint the “plateau” of the relationship. The spreadsheet allowed us to quickly and accurately calculate the minimum and maximum radius values, along with the full range, with different combinations of theta values. An example is given below.

Link	Length	Theta_12_min	30
1	7	Theta_12_max	120
2	7	Theta_5_max	45
3	5	Theta_3	20
4	5	Theta_35	-15
5	7		
r_min	1.740303		
r_max	9.910691		
Range_x	9.899495		

By inserting various combinations of link sizes into the spreadsheet, we observed a preliminary viable option. It gave us a large workable area while not overly extending the length of the links, and happened when both links 1 and 2 are equal in length and measure 7 cm. Our next task was to perform a sensitivity analysis and verification of this preliminary result, and we did that using Matlab.

First, we plotted the combined weight of 7 links versus the length of each link. This is done by assuming a rectangular slab for each link and the following formula:

$$W = 7 * (\text{Link Length})(2\text{cm})(1\text{cm}) \left(8.03 \frac{\text{g}}{\text{cm}^3}\right) \left(0.0022046 \frac{\text{lb}}{\text{g}}\right)$$



Based on the user satisfaction curve vs. the device total weight, we should not go beyond 5 lb for the device as a whole. Thus, the links alone, without the motors, encoders and other equipment, should not be more than approximately 2 lb – corresponding to around a 7 cm link length. This verifies that the preliminary result of a 7 cm link size does not conflict our weight requirements. However, we must still check whether it conflicts with our workable area requirements. To check that the link lengths which fall below the maximum acceptable weight also give us an acceptable workable area, we plot the mathematical range relationship in Matlab. The following workable area relations are entered:

$$L_R^2 = L_1^2 + L_2^2 - 2 L_1 L_2 \cos \theta_{12}$$

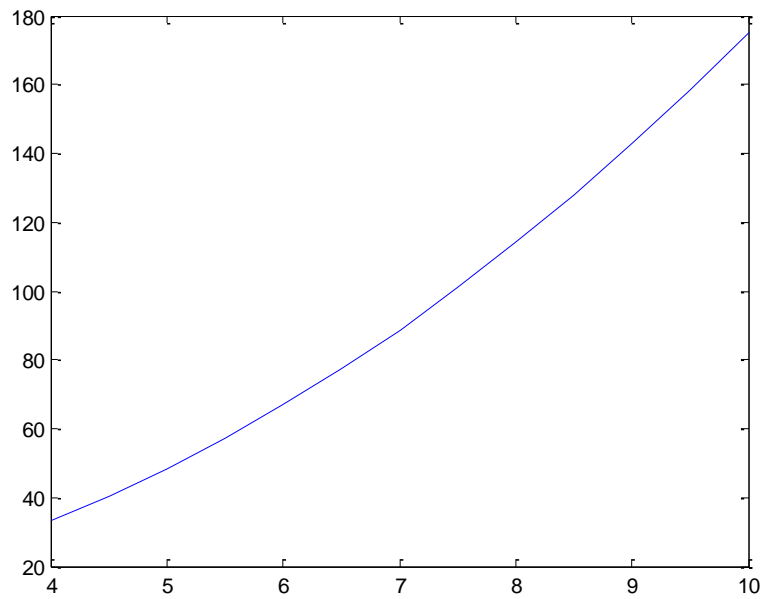
$$L'_5 = L_5 \cos \theta_5$$

$$z = L_R + L_3 \cos \theta_3 - L'_5 \cos (90 - \theta_3 - \theta_{3-5})$$

$$y = -L_3 \cos \theta_3 + L'_5 \cos (90 - \theta_3 - \theta_{3-5})$$

$$R = \sqrt{z^2 + y^2}$$

Plotting the workable area range versus the link size, we get the following graph. On the plot, a link size of 7 cm corresponds to a workable range of approximately 90 mm, or 9 cm. This value is greater than the standard implant size that we aim to achieve, thus, a link size of 7 cm is both acceptable for maximum weight constraints and minimum workable area constraints.



The Matlab code for the analysis described above can be found in the Appendix.

```
>> y = x.^2 + x.^2 - 2.*x.*x.*cos(30) + 5*cos(20) - 7*cos(45)*cos(90-20+15);
>> z = y;
>> y = -5*cos(20) + 7*cos(45)*cos(90-20+15);
>> R = sqrt(z.^2 + y.^2);
>> plot(x,R)
>> density = 8.03;
>> conversion = .0022046;
>> weight = x*2*1*density*conversion;
>> f = 7.*weight;
>> plot(x,f)
>> plot(x,f)
```

Appendix C: Testing Procedures

The testing procedures for the Praxia user and precision/accuracy tests are included here.

Step	Task	Comments
1.	<div>Mill Calibration Positions</div> <div><div><div>1.</div><div>Clamp an approximately 6cm by 6cm by 1cm piece of scrap carbon steel in the mill vice.</div></div><div><div>2.</div><div>Use edge finder tool to position the mill at a corner of the steel. Replace edge finder with a 0.2mm drill bit and reposition the z-coordinate at the surface of the device. Zero all dimensions.</div></div><div><div>3.</div><div>Use the mill to make holes 1mm deep holes at four positions [(40mm, 40mm); (40mm, 10mm); (10mm, 40mm); (10mm, 10mm)]</div></div><div><div>4.</div><div>Clamp steel in a vertical orientation and complete steps 1.2 and 1.3 at [(5mm, 10mm); (5mm, 40mm)]</div></div></div>	Try to drill each hole quickly and use coolant to avoid heating metal excessively. Actual position of calibration points may vary. Record any changes on the testing procedure.
2.	<div>Create holes for bone mount</div> <div><div><div>1.</div><div>On a flat surface of the steel create two 5mm holes 10mm apart using a 2.5mm drill bit.</div></div><div><div>2.</div><div>Tap the holes using a 3.3mm tap</div></div></div>	
3.	<div>Device Precision</div> <div><div><div>1.</div><div>Connect device to carbon steel piece designed above through the bone mount using two m3 screws</div></div><div><div>2.</div><div>Connect a pin to the tool end so that the pin head is positioned at the centre of the radius of curvature of the tool.</div></div><div><div>3.</div><div>Place the tool at the calibration corner of the steel piece and record the encoder determined position.</div></div></div>	

	4.	Place the tool at the marks located at [(40mm, 40mm); (40mm, 10mm); (10mm, 40mm); (10mm, 10mm)] and record the encoder determined position.	
	5.	Place the tool at the marks located at [(5mm, 10mm); (5mm, 40mm)] in the vertical plane and record the encoder determined position.	
4.	Device Accuracy		
	1.	Repeat step 3 five times	
	2.	Graph the actual mark positions as well as each test position.	
5.	Workable Area		This test does not determine the volume of the device, but provides a basic footprint range and will verify that the device will be effective for the implant sizes considered.
	1.	Position tool at the calibration corner with a piece of paper positioned below the steel piece.	
	2.	Trace the tool head through each of the steel marks and ensure the tool head does not leave the surface of the steel piece. Can this be completed effectively?	
	3.	Move the tool head towards each of the corners of the piece of paper. Record the device reach to each of the corners on the piece of paper.	
	4.	Keeping the x and y coordinates the same as step 5.3 record the highest possible vertical position.	

Step	Task	Comments
6.	Hard Surface	Tool should not penetrate the hard surface.
	1. Clamp a piece of foam to the steel testing piece created in step 1.	
	2. Implement four models into the system (flat, spherical bulge, cone and pyramid)	

	3.	Slowly trace the surface of the foam for each of the shapes, removing excess material and revealed the implemented shape. Not down any positions where the tool head penetrates the hard surface	
	4.	Place the tool head at any corners. Access the stability of the tool at these locations.	
7.	Instability		Tool instability should be maintained to within +/- 1mm.
	1.	For each of the shapes implemented above place the tool head at any corners. Access the stability of the tool at these locations.	

Step	Task		Comments	
8.	Virtual Weight		Testing using foam will not provide the same resistance as a bone, but be used to assess the effects of the weight of the device on the user in different orientations while performing surgical type operations. The user assessment scale is based on the user’s perceived control over the position of the device and the user’s ability to maneuver the tool along a specific path.	
	1.	For each user: Setup device using foam and implement a hemi spherical hard surface. The foam must be cut to within 5mm of the hard surface prior to testing.		
	2.	With a black pen, place point pairs 5cm apart in a zigzag pattern at 1 cm intervals and mark transition paths across the surface points – use a total of 10 points.		
	3.	In an orientation perpendicular to the step 8.2, repeat step 8.2.		
	4.	Position user 45 degrees from the bone mount position and a line connecting the hip and the knee.		
	5.	Make user follow the zigzag paths described in 8.2 and 8.3, pausing at each point for 5 seconds. Each transition should take between 3 and 5 seconds.		
6.	Ask user to rate the device performance based on the scale shown in step 8			

		comments.	6.																							
	7.	Ask user to provide general comments on the perceived effectiveness of the device for high precision cutting applications.	7.	Device is comfortable to hold, follows desired path well and can maintain position with limited input																						
	8.	Measure and record the maximum error between the cut path and desired path.	8.																							
			9.	Device is comfortable to hold, follows desired path well and can maintain position without user input																						
			10.	Device does not affect user control of the tool.																						
9.	Accessibility		This assessment should be completed by experienced surgeons.																							
	1.	For each user: Setup device using foam and implement a hemi spherical hard surface. The foam must be cut to within 5mm of the hard surface prior to testing.	<table><tr><th>Rating</th><th>Description</th></tr><tr><td>1.</td><td>Device is does not provide access critical locations</td></tr><tr><td>2.</td><td></td></tr><tr><td>3.</td><td></td></tr><tr><td>4.</td><td></td></tr><tr><td>5.</td><td>Device is allows access the all critical locations, but requires undesirable repositioning of hand</td></tr><tr><td>6.</td><td></td></tr><tr><td>7.</td><td></td></tr><tr><td>8.</td><td></td></tr><tr><td>9.</td><td></td></tr><tr><td>10.</td><td>Device provides comfortable access to all desired areas.</td></tr></table>		Rating	Description	1.	Device is does not provide access critical locations	2.		3.		4.		5.	Device is allows access the all critical locations, but requires undesirable repositioning of hand	6.		7.		8.		9.		10.	Device provides comfortable access to all desired areas.
Rating	Description																									
1.	Device is does not provide access critical locations																									
2.																										
3.																										
4.																										
5.	Device is allows access the all critical locations, but requires undesirable repositioning of hand																									
6.																										
7.																										
8.																										
9.																										
10.	Device provides comfortable access to all desired areas.																									
	2.	With a black pen, place point pairs 5cm apart in a zigzag pattern at 1 cm intervals and mark transition paths across the surface points – use a total of 10 points.																								
	3.	In an orientation perpendicular to the step 8.2, repeat step 8.2.																								
	4.	Position user 45 degrees from the bone mount position and a line connecting the hip and the knee.																								
	5.	Make user follow the zigzag paths described in 9.2 and 8.3, pausing at each point for 5 seconds. Each transition should take between 3 and 5 seconds.																								
	6.	Ask user to rate the device performance based on the scale shown in step 9 comments.																								
	7.	Ask user to provide general comments on the																								

		perceived effectiveness of the device for high precision cutting applications.	
	8.	Measure and record the maximum error between the cut path and desired path.	

Appendix D: Manufacturing Drawings

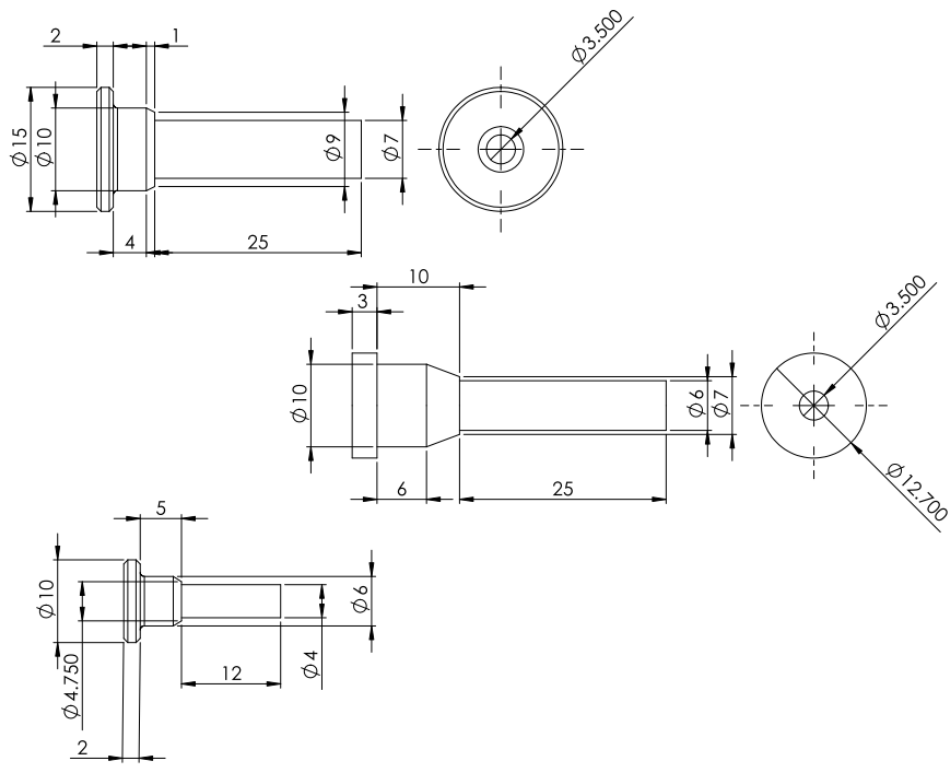


Figure 13: Axle drawings to be machined on a lathe

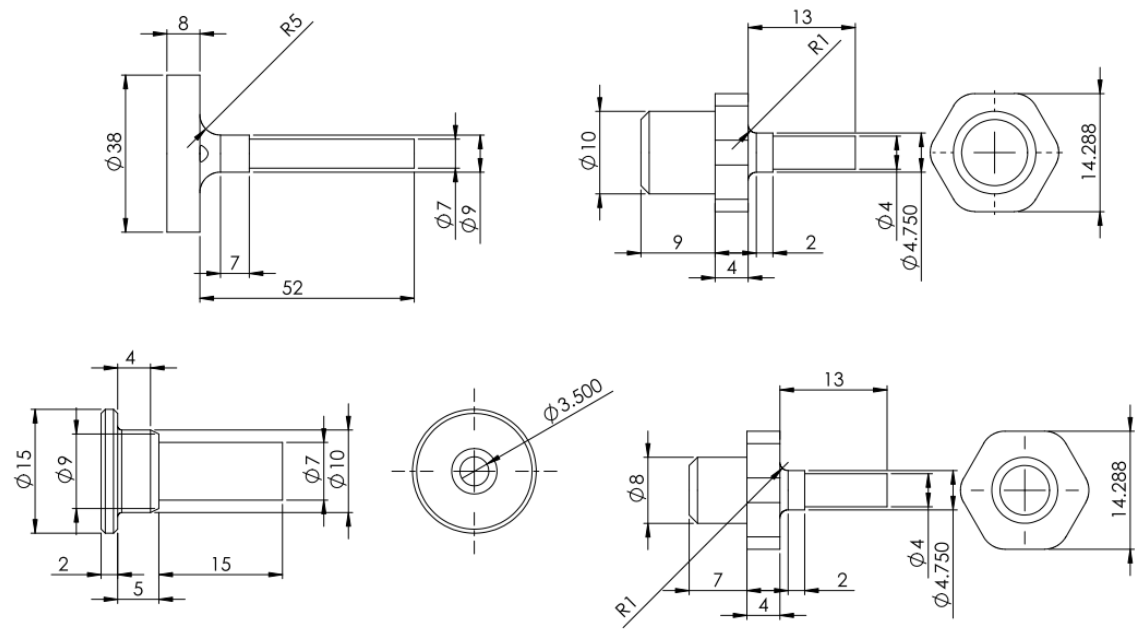


Figure 14: Additional axle drawings to be machined on a lathe

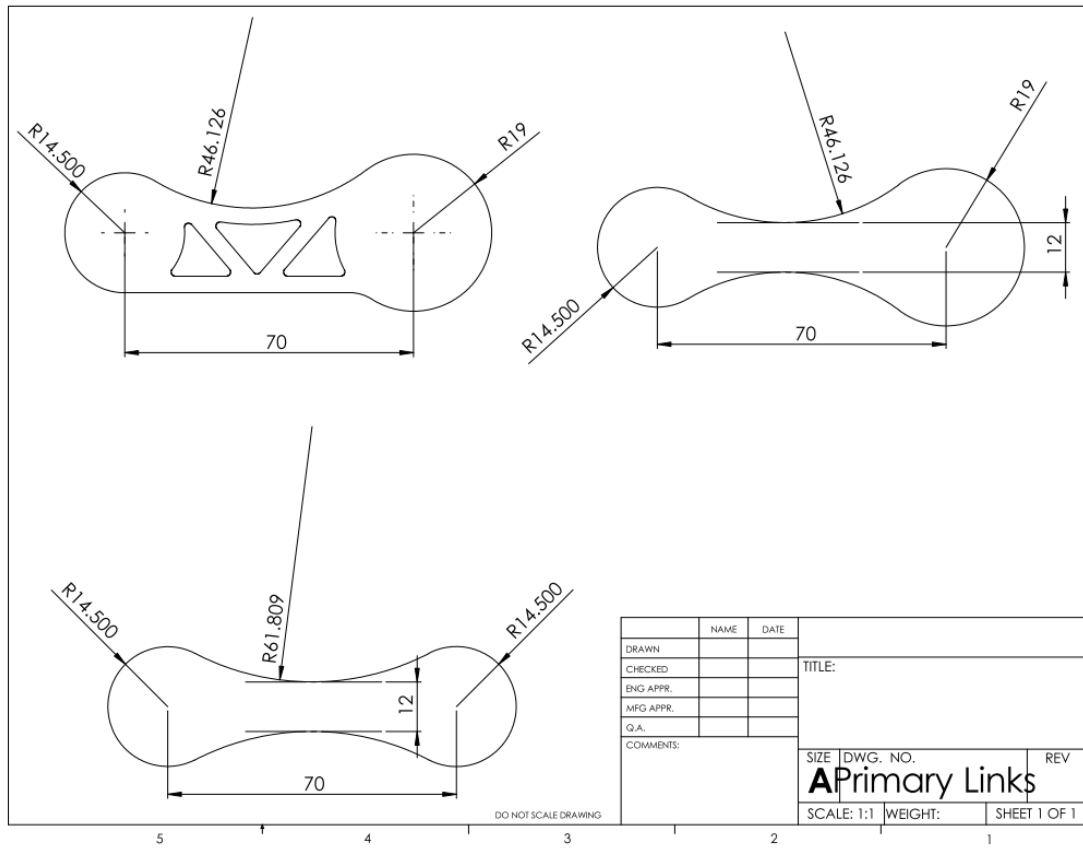


Figure 15: Link drawings to be water jet cut and drilled on a mill

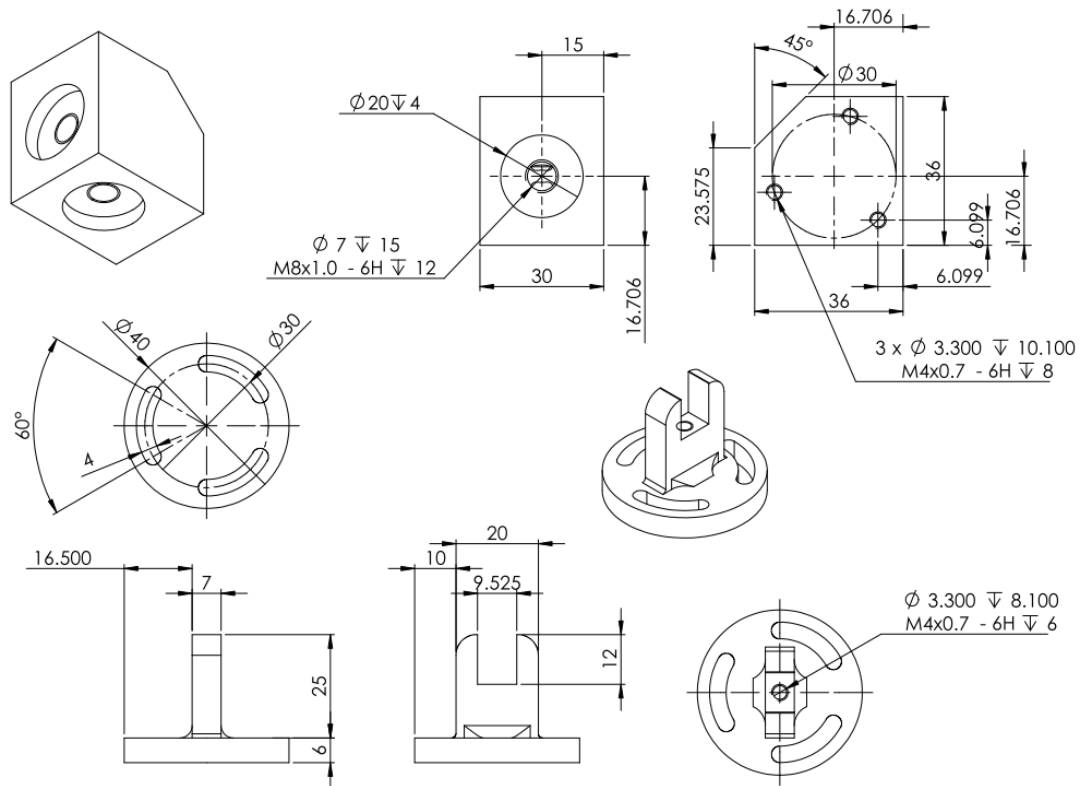


Figure 16: The rotating base drawings and vertical offset link designed to be milled

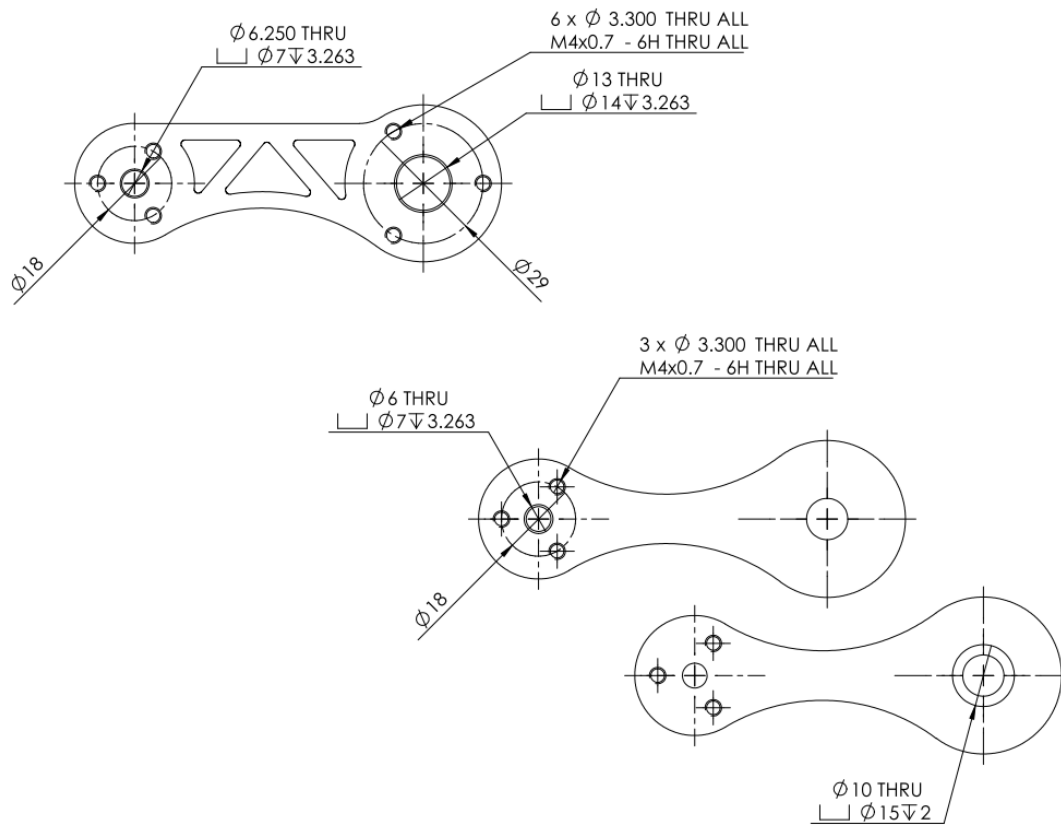


Figure 17: Primary links to be water jet cut and machined on a mill

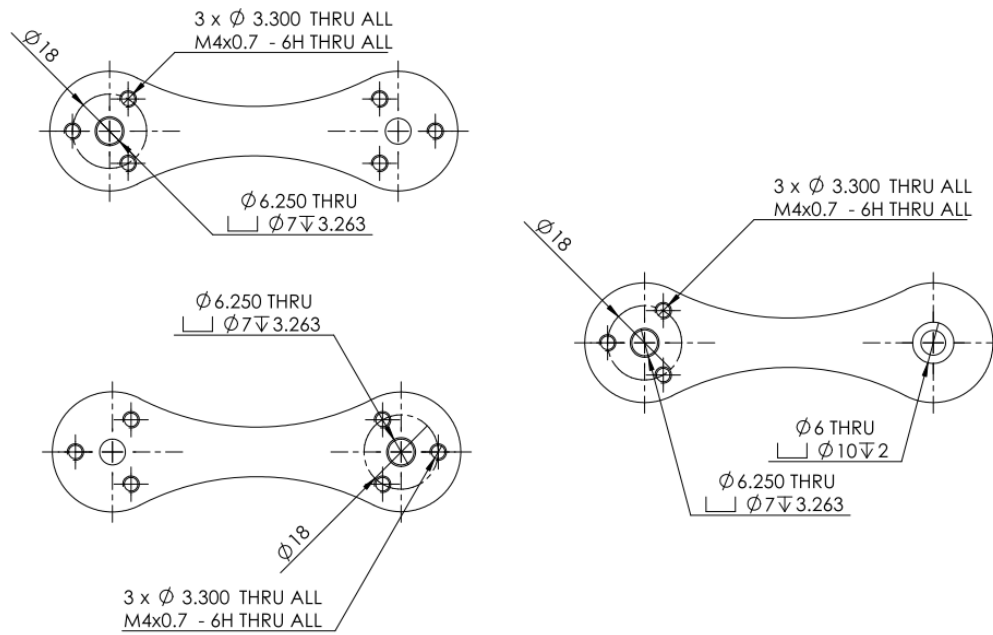


Figure 19: Secondary links designed to be water jet cut and drilled on a mill

Appendix E: Encoder Specifications



page 1 of 5
date 01/2009

PART NUMBER: AME

DESCRIPTION: modular incremental encoder

The AME Series are high performance, low cost, 2 channel optical incremental encoders. Each encoder contains a LED source, an integrated circuit with detectors and circuitry, and an optical disc which rotates between the emitter and detector IC. These encoders can be quickly and easily mounted to a motor.



ELECTRICAL SPECIFICATIONS

output waveform	Square wave
output signals	A, B phase
output voltage	H: $\geq 85\% V_{cc}$ L: $\leq 0.3 V$
current consumption	$\leq 25 \text{ mA}$
output phase difference	$90^\circ \pm 45^\circ$
supply voltage	5 V dc
output resolution (ppr)	100, 200, 256, 360, 400, 500, 512, 1000, 1024
frequency response	20 kHz (voltage output), 50kHz (line driver output)
output current	0~5 mA

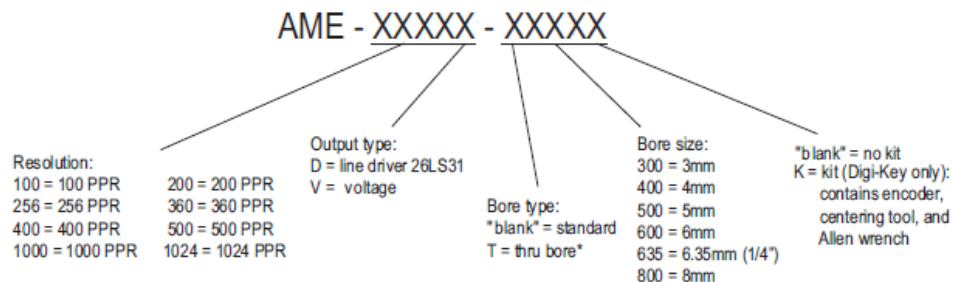
MECHANICAL SPECIFICATIONS

rotor inertia of code-wheel	$6.0 \times 10^{-8} \text{ kgm}^2$
hollow shaft diameter	$\leq \varnothing 8 \text{ mm}$
shock resistance	980 m/s^2 , 6ms, 2 times each on XYZ
vibration proof	50 m/s^2 , 10~200 Hz, 2 hours each on XYZ
working life	MTBF $\geq 5000\text{h}$ (+25°C, 2000rpm)
weight	10g (with 0.5 meter cable)

ENVIRONMENTAL SPECIFICATIONS

operating temp	-25° to +85° C
storage temp	-40° to +100° C
humidity	30~85% no condensation
protection	IP50

ORDERING INSTRUCTIONS

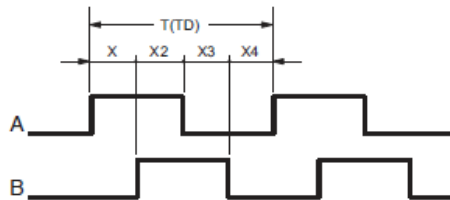


*Removing the cap which covers the bore will turn the Standard style into a Thru Bore style

20050 SW 112th Ave. Tualatin, Oregon 97062 phone 503.612.2300 fax 503.612.2383 www.cui.com

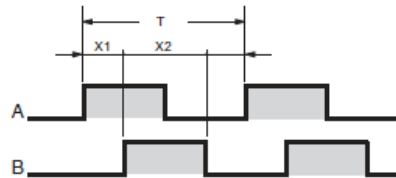
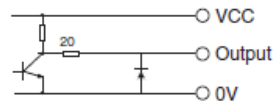
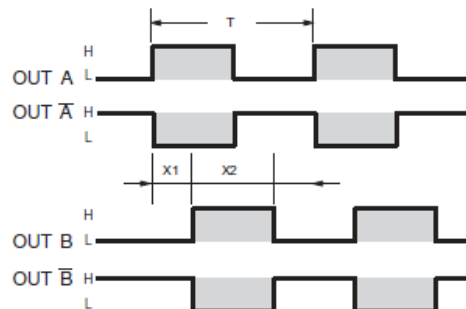
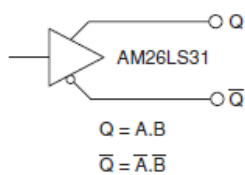
PART NUMBER: AME

DESCRIPTION: modular incremental encoder

OUTPUT WAVEFORM


- Square-wave accuracy: $X_1 + X_2 = 1/2T \pm 1/12T$
 $X_3 + X_4 = 1/2T \pm 1/12T$
- Pitch error of period: $\pm 0.01T$
- Pitch error of phase position: $\leq 1/18T$
- Z phase: $T_z = 1/4T$ (1T, 1/2T, 1/4T...)
- Period of pulses: $T = 360^\circ / N$ (N: output pulses)
- Signal accuracy: $X_n = 1/4T \pm 1/12T$ (n=1, 2, 3, 4)

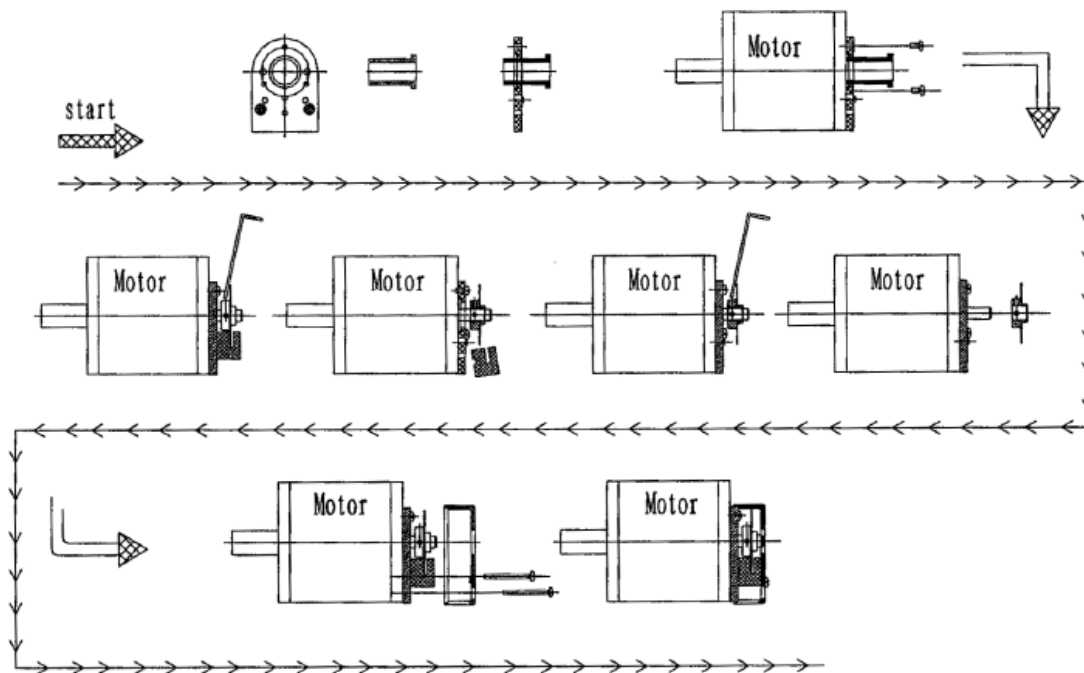
A leads B clockwise when viewing the encoder shaft end.
The position of Z phase against A, B phase is not specified.

Voltage output

Line driver output


PART NUMBER: AME

DESCRIPTION: modular incremental encoder

INSTALLATION DRAWING



Light Duty Incremental Encoders

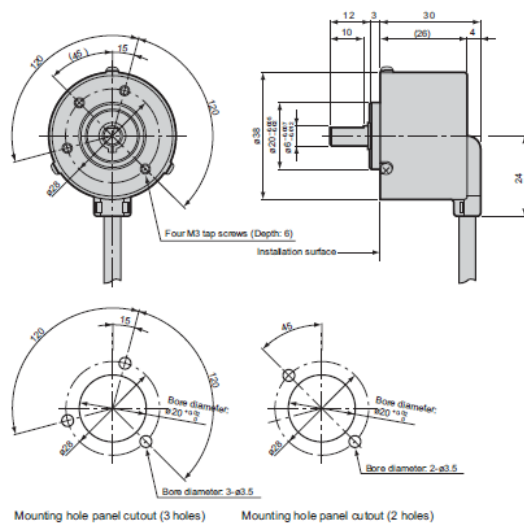
Specifications

Electrical Specifications				
Model			TRD-Sxxxx-BD TRD-SHxxxxBD (open collector)	TRD-Sxxxx-VD TRD-SHxxxxVD (line driver)
Power Supply	Operating Voltage		10.8 - 26.4VDC*	+4.75 - 5.25VDC*
	Allowable Ripple		3% max.	-
	Current Consumption		50 mA max.	
Signal Waveform			Two-phase + home position	
Max. Response Frequency			200kHz	
Duty Ratio			50 ± 25%	
Phase Difference Width			25 ± 12.5%	
Signal Width at Home Position			100 ± 50%	
Output	Rise/Fall Time		1µs max. (when cable length is 1m)	-
	Output Type		NPN open collector output, sinking	Line driver output (26C31 or equivalent)
	Output Logic		Negative logic (active low)	Negative logic (active high)
	Output Current	H	-	2.5 V min.
	Output Voltage	L	0.4 V max.	0.5 V max.
	Influx Current		30mA max.	-
	Load Power Voltage		35 VDC max.	-
	Short-Circuit Protection		Between output and power supply	
* To be supplied by Class II source				
Mechanical Specifications				
Starting Torque		Max. 0.001 Nm (.00074 ft./lbs)		
Max. Allowable Shaft Load		Radial: 20N (4.5 lbs) Axial: 10N (2.25 lbs)		
Max. Allowable Speed		6000 rpm (highest speed that can support the mechanical integrity of encoder)		
Wire Size		AWG26		
Weight		Approx. 150g (5.3 oz) with 2m cable		
Environmental Specifications				
Ambient Temperature		10 to 70°C; 14 to 158°F		
Storage Temperature		-25 to 85°C; -13 to 185°F		
Operating Humidity		35-85% RH		
Voltage Withstand		500VAC (50/60Hz) for one minute		
Insulation Resistance		50MΩ min.		
Vibration Resistance		Durable for one hour along three axes at 10 to 55 Hz with 0.75 amplitude		
Shock Resistance		11 ms with 490 m/s² applied three times along three axes		
Protection		IP40: dust proof		

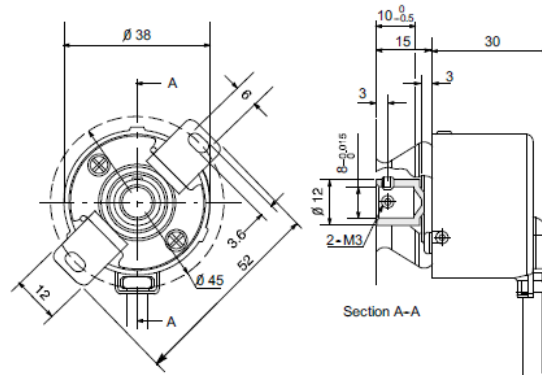
Light Duty Incremental Encoders

Dimensions

Standard shaft models



Hollow shaft models

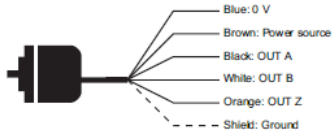


All dimensions in mm
1mm = 0.03937in

Wiring diagrams

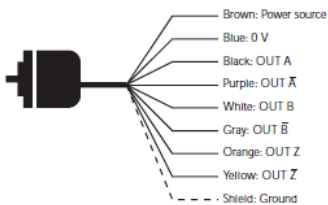
Open collector connections

Cable shield is not connected to the encoder body; enclosure is grounded through the 0V wire



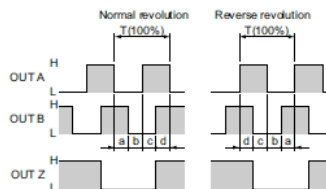
Line driver connections

Cable shield is not connected to the encoder body; enclosure is grounded through the 0V wire

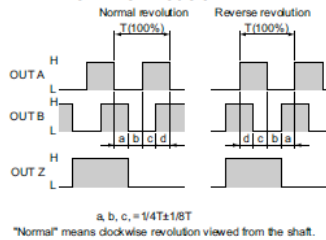


Channel timing charts

Open Collector Models



Line Driver Models



a, b, c, = 1/4T ± 1/8T

"Normal" means clockwise revolution viewed from the shaft.

How to read the timing charts

Open Collector Models

Out A and Out B are 90 degrees out of phase. Like any quadrature encoder, four unique logic states are created internally to the encoder. This is based on the rising edge to rising edge (one cycle) on channel A or B that indicates one set of bars on the internal encoder disk has passed by the optical sensor.

OUT Z is the absolute reference added to an incremental encoder and is also known as home position. It signifies a full rotation of the encoder disk.

Line Driver Models

Channel A (OUT A and A-not) and Channel B (OUT B and B-not) are also 90 degrees out of phase on line driver encoders. OUT Z is the same as on open collector models, and is the absolute reference (home position). It signifies one full rotation of the encoder.